Heterodinuclear Cryptates $[EuML(dmf)](ClO_4)_2$ (M = Ca, Cd, Ni, Zn): Tuning the Luminescence of Europium(III) through the Selection of the Second Metal Ion

Qiu-Yun Chen,[a, b] Qin-Hui Luo,*[a, b] Xue-Lei Hu,[a, b] Meng-Chang Shen,[a] and Jiu-Tong Chen[c]

Abstract: Four heterodinuclear cryptates $[EuML(dmf)](ClO_4)_2$ (M = Ca, Cd, Ni, Zn) were synthesized by a two-step method (L denotes deprotonated anionic cryptand synthesized by condensation of tris(2-aminoethyl)amine with 2,6-diformyl-4-chlorophenol). The ES-MS spectra of the four cryptates and the crystal structure of $[EuNiL(dmf)](ClO_4)_2 \cdot MeCN$ confirm that a strict dinuclear $Eu^{III}-M^{II}$ entity exits in the cryptates. The cyclic voltammetry and luminescence spectral investigations indicate that the introduction of second metal ions into the mononuclear Eu^{III} cryptate result in a negative shift of the redox potential of Eu^{III} and a change in luminescence intensity of Eu^{III}. The cryptate $[EuML(dmf)](ClO_4)_2$ was shown to quench the emission of Eu^{III} when M = Ni and to enhance the emission of Eu^{III} when M = Ca, Cd, and Zn in the sequence: mononuclear < Eu – Ca < Eu – Cd < Eu – Zn.

Keywords: cryptates · europium · lanthanides · luminescence · structure elucidation

Introduction

Over recent years the interest in the synthesis and properties of lanthanide complexes has increased dramatically.[1–6] Their novel structures and properties have resulted in technological applications,[7–9] for example, lanthanide(III) complexes are important as tunable photonic devices with potential for biomedical diagnostics and fluorescence imaging[10] as well as chemical logics[11] in molecular information processing. Some lanthanide ions, such as Eu^{3+} and Tb^{3+}, exhibit strong emission and excited states with long lifetimes but have extremely low absorption coefficients[12] and so the scope of their application is limited. This drawback can be overcome through encapsulation of metal ions inside the cavity of cryptands. The cryptands shield the metal ions from interaction with solvents and thus avoid radiationless deactivation processes of luminescence emission and enhance thermodynamic and kinetic stability of the complexes in solution by the cryptate effect. Therefore, europium or terbium cryptates with valuable luminescence properties can be obtained by a suitable choice of cryptand with an antenna chromophore[13] and by tuning the photophysical and electronic properties through structural modifications of the cryptates.[14, 15] The syntheses and luminescence properties of some Eu^{III} cryptates have been described,[16–21] such as those based on oxamacrocycles,[22, 23] azamacrocycles,[24] macrocycles with bipyridyl[25, 26] and aromatic *N*-oxide functional groups,[27] and macrocycles with functionalized calixarenes,[28] as well as novel iminophenolate cryptates[29, 30] (Robson type).

However, the number and type of cryptates that have been used is still quite limited.[31] All of them are mononuclear or homodinuclear lanthanide cryptates. There have been few reports on the luminescence properties of heterodinuclear cryptates containing both lanthanide(III) and other metal ions. It is well known that heterodinuclear complexes have unique properties that are different from those of the analogous mononuclear and homodinuclear complexes. Introduction of a second, dissimilar, metal ion into mononuclear lanthanide complexes permits the tuning of magnetic[15] and photophysical properties of lanthanide ions.[32] Recently a Robson-type heterodinuclear Dy – Cu cryptate was synthesized by our group for the first time.[33] Subsequently, the magnetic interaction between Gd^{III} and Ni^{II} atoms in the iminophenolate Gd – Ni cryptate[34] was studied. As part of a continuing study aimed at gaining a better understanding of the

[a] Prof. Q.-H. Luo, Dr. Q.-Y. Chen, X.-L. Hu, M.-C. Shen
Coordination Chemistry Institute
State Key Laboratory of Coordination Chemistry
Nanjing University
Nanjing, 210093 (P. R. China)
Fax: (+86) 25-3317761
E-mail: qhluo@jlonline.com

[b] Prof. Q.-H. Luo, Dr. Q.-Y. Chen, X.-L. Hu
State Key Laboratory of Lanthanide Chemistry
Beijing University
Beijing (P. R. China)

[c] J.-T. Chen
FuZhou State Key Laboratory of Structure Chemistry
FuZhuo (P. R. China)

  0947-6539/02/0817-3984 $ 20.00+.50/0

luminescence properties of lanthanide heteronuclear cryptates, herein we report four new heterodinuclear europium(III) cryptates $[EuML(dmf)](ClO_4)_2$ (M = Ca, Cd, Ni, Zn; L denotes deprotonated anionic cryptand synthesized by condensation of tris(2-aminoethyl)amine with 2,6-diformyl-4-chlorophenol). The synthetic route to these compounds is different from the general method for Robson-type heterodinuclear dimensional macrocyclic complexes and is shown in Scheme 1.[35] They were characterized by electrospray mass spectrometry (ES-MS), cyclic voltammetry (CV), and X-ray crystal structure analysis. Their luminescence properties were also studied. The experimental results show that introduction of the second metal ion into the mononuclear Eu^{III} cryptate resulted in an increase of the absorption coefficients of the cryptates, a negative shift of the redox potential of Eu^{III}, and a change in the luminescence intensity of Eu^{III}. The intensity can be tuned by selective introduction of the second metal ion into the mononuclear Eu^{III} cryptate.

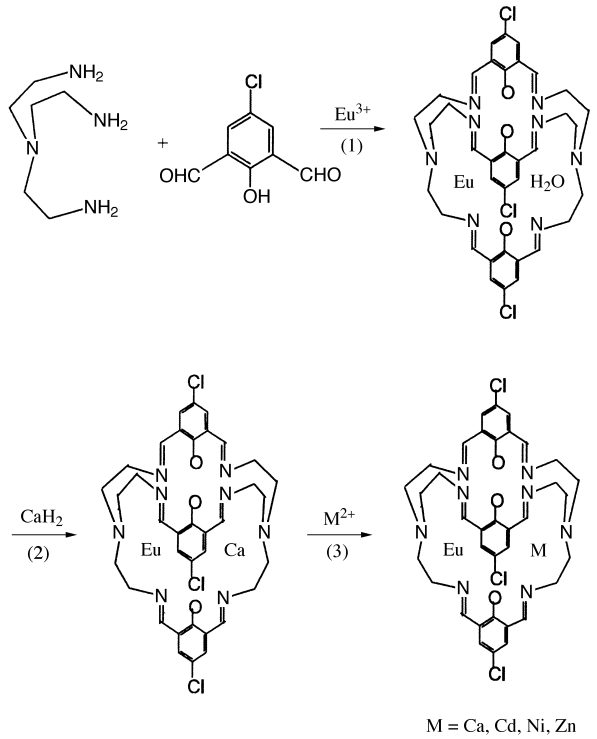

Scheme 1. The syntheses of the heterodinuclear cryptates. The electron charges of metal and cryptate cations are omitted.

Results and Discussion

Syntheses: In general,[35] Robson-type heteronuclear two-dimensional macrocyclic complexes are obtained by a [2+1] condensation of dialdehyde with amine in the presence of the first metal and then by cyclization with another molecule of dissimilar amine using the second metal as a template. The present cryptates $[EuML(dmf)](ClO_4)_2$ (M = Ca **1**, Cd **2**, Ni **3**, Zn **4**) were synthesized by the following route as shown in Scheme 1: 1) Synthesis of $[Eu(H_3L)(NO_3)(H_2O)](ClO_4)_2$ (**5**) as the precursor which included one molecule of water as a guest species in the cavity. 2) During the reaction of added CaH_2 with the precursor, three protons of the cryptand were neutralized and the included water molecule was replaced by a calcium ion, which led to the formation of the $[EuCaL]^{2+}$ ion as an intermediate in solution that could be isolated as the product $[EuCaL(dmf)](ClO_4)_2$. 3) The ES-MS of $[EuCaL(dmf)](ClO_4)_2$ has demonstrated that the Ca^{2+} ion in the cryptate is unstable and labile towards dissociation and replacement. Thus the Ca^{2+} ion may be replaced by transition metals. Thus far we failed to synthesize d–f heteronuclear cryptates in the absence of CaH_2 or by the general method.

Characterization: The values of the solution molar conductivities of cryptates **1**–**4** indicated that all are 1:2 electrolytes. The results of molar conductivity studies and elemental analysis showed that three phenolic protons of mononuclear cryptate $[Eu(H_3L)(NO_3)(H_2O)](ClO_4)_2$ (**5**) were lost during coordination of the second metal ion, in agreement with the X-ray structural determination. The data from the electronic spectra are presented in Table 1. Electronic spectra of heterodinuclear cryptates in MeCN display three intense bands. The band centered around 380 nm is assigned to the C=N chromophore, whereas the other two bands at about 250 nm and 225 nm are assigned to the $\pi-\pi^*$ transition of the K band of benzene rings. In the Eu–Ni cryptate, the remaining band at 650 nm may be assigned to the d–d transition of Ni^{II}. The introduction of a second metal ion into $[Eu(H_3L)(NO_3)(H_2O)](ClO_4)_2$ led to a blue shift of the three intense bands and to an increase of the molar absorption coefficients. The maximum blue-shift of the C=N bands observed is 30 nm, and the maximum increase of the molar absorption coefficient of the C=N band is about $9\times10^3\,L\,mol^{-1}\,cm^{-1}$.

Electrospray mass spectra: The ES-MS data of cryptates **1**–**4** are listed in Table 2. The most intense peak of each of the heteronuclear cryptates corresponds to the fragment $[EuML]^{2+}$ formed by loss of a coordinated DMF molecule. This confirms the presence of the $Eu^{III}-M^{II}$ core in the cryptate. The other peak clusters are assigned to binding of the fragment $[EuML]^{2+}$ with solvent molecules or ClO_4^-, or loss of chlorine atoms from the phenyl rings. Unlike for cryptate **1**,

Table 1. Data from the electronic spectra of Eu^{III} cryptates in MeCN solution.

No	cryptates	λ [nm] (ε)	λ [nm] ($\varepsilon\times10^4\,L\,mol^{-1}\,cm^{-1}$)	
$[EuCaL(dmf)](ClO_4)_2$ (**1**)		380 (2.07)	247 (8.84)	222 (9.21)
$[EuCdL(dmf)](ClO_4)_2$(**2**)		376 (2.50)	247 (9.42)	224 (10.01)
$[EuNiL(dmf)](ClO_4)_2\cdot MeCN$ (**3**)	635(33)	377 (1.88)	248 (7.03)	225 (8.33)
$[EuZnL(dmf)](ClO_4)_2\cdot MeCN$ (**4**)		379 (2.46)	248 (8.96)	223 (9.75)
$[Eu(H_3L)(NO_3)(H_2O)](ClO_4)_2$ (**5**)		406 (1.62)	264 (3.04)	230 (8.30)

  0947-6539/02/0817-3985 $ 20.00+.50/0

Table 2. The assignment of ES-MS peaks for cryptates **1**–**4** in MeOH.

Cryptate	Peaks (m/z)	Assignments
1	1027.3 (37)	$[EuCaL + ClO_4^-]^{2+}$
	479.3 (14)	$[EuCaL + CH_3OH]^{2+}$
	463.3 (100)	$[EuCaL]^{2+}$
	444.4 (37)	$[EuL + 2H^+]$
2	1099.0 (12)	$[EuCdL + ClO_4^-]^+$
	500.4 (100)	$[EuCdL]^{2+}$
3	1043.3 (8)	$[EuNiL + ClO_4^-]^+$
	1003.1 (20)	$[EuNi(L - 3Cl) + ClO_4^- + 1.5MeOH + H_2O]^+$
	985.3 (20)	$[EuNi(L - 3Cl) + ClO_4^- + 1.5MeOH]^+$
	472.3 (100)	$[EuNiL]^{2+}$
	464.3 (25)	$[EuNi(L - Cl) + H_2O]^{2+}$
4	1051.2 (18)	$[EuZnL + ClO_4^-]^+$
	512.2 (10)	$[EuZnL(dmf)]^{2+}$
	476.3 (100)	$[EuZnL]^{2+}$

no peaks were found due to the loss of Eu^{3+} or M^{2+}. This indicates that cryptates **2**–**4** are stable under the conditions of ES-MS. From Table 2, it is remarkable to note that the peak in the ES-MS of $[EuCaL(dmf)](ClO_4)_2$ (**1**) at m/z 404.4 is attributed to the species $[EuL+2H^+]^{2+}$ which was formed by loss of the encapsulated Ca^{2+} ion and the trapping of two protons. This indicates that cryptate **1** is unstable and labile; the encapsulated Ca^{2+} ion is able to dissociate and be replaced by transition metal ions as mentioned in the previous section. The isotopic distribution at m/z 463.3 was calculated[36] by using the numbers and natural isotopic abundance of atoms in $[EuCaL]^{2+}$. The calculated pattern (Figure 1a) is similar to the experimental one (Figure 1b), further confirming the the existence of the heterodiuclear Eu^{III}–Ca^{II} cryptate.

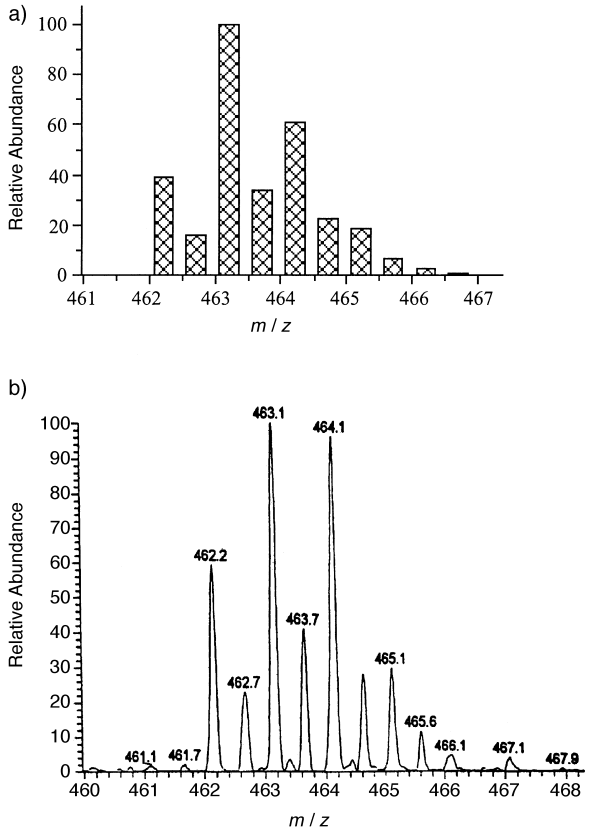

Figure 1. The isotopic distribution of the peak cluster at m/z 463.3: a) calculated pattern; b) experimental pattern.

Cyclic voltammetric behavior: The cyclic voltammogram of $[Eu(H_3L)(NO_3)(H_2O)](ClO_4)_2$ (**5**) in DMF, scanned from 0 – – 2.20 V at a scan rate of 0.05 V s^{-1} (Figure 2a), shows one pair of well-defined cathodic and anodic peaks with peak potentials of $E_{pc} = -0.860$ and $E_{pa} = -0.780$ V (NHE), respectively.

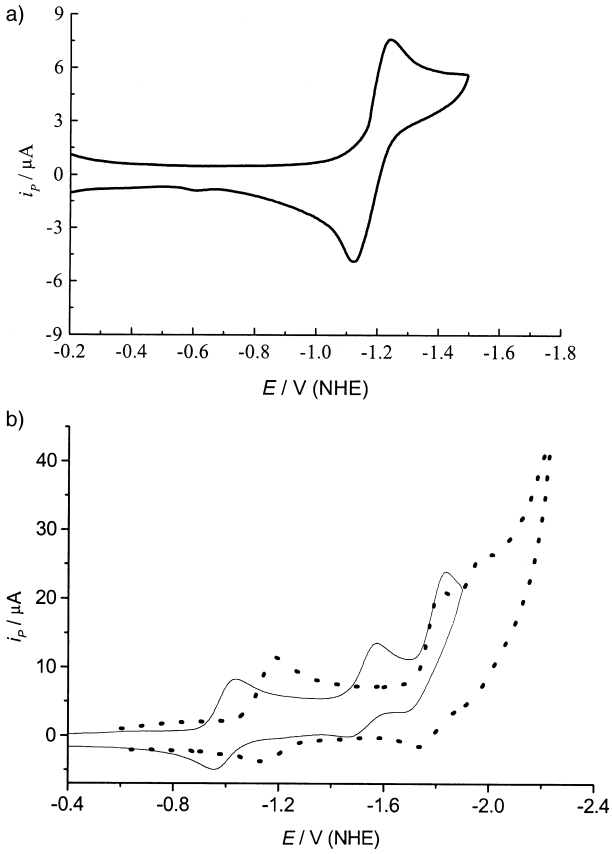

Figure 2. The cyclic voltammograms of a) $[Eu(H_3L)(NO_3)(H_2O)](ClO_4)_2$ (**5**), b) $[EuNiL(dmf)](ClO_4)_2$ (**3**; full line) and $[EuZnL(dmf)](ClO_4)_2$ (**4**; dash line) in DMF, concentration of the complexes: 1.50×10^{-3} mol L^{-1}, Bu_4NClO_4: 0.1 mol L^{-1}, scan rate: 0.05 V s^{-1}.

The value of the half-wave potential $E_{1/2}{}^1$ was calculated to be – 0.820 V. The cathodic and anodic peaks are of equal intensity and the separation between the anodic and cathodic peaks (80 mV) increases with scan rate. Furthermore, peak heights for the complex are proportional to the square root of the scan rate. From these results, it may be concluded that cryptate **5** underwent a quasi-reversible reduction process that can be ascribed to the Eu^{III}/Eu^{II} couple. The voltammograms of heterodinuclear cryptates **3** and **4** are shown in Figure 2b. Cryptate **2** also has a voltammetric pattern similar to those of **3** and **4**. For example, $[EuNiL(dmf)]^{2+}$ exhibits three one-electron redox processes that may be assigned as follows:

$$[Eu^{III}Ni^{II}L]^{2+} + e \rightarrow [Eu^{II}Ni^{II}L]^+ \; E_{1/2}{}^1 = -0.990 \text{ V}$$

$$[Eu^{II}Ni^{II}L]^+ + e \rightarrow [Eu^{II}Ni^{I}L]^0 \; E_{1/2}{}^2 = -1.520 \text{ V}$$

$$[Eu^{II}Ni^{I}L]^0 + e \rightarrow [Eu^{II}Ni^{0}L]^- \; E_{1/2}{}^3 = -1.765 \text{ V}$$

The electrochemical data of the four cryptates **2**–**5** are listed in Table 3. Notably, in the three heteronuclear cryptates,

0947-6539/02/0817-3986 $ 20.00+.50/0 *Chem. Eur. J.* **2002**, *8*, No. 17

Table 3. The half wave potentials [V] of some Eu^{III} cryptates in DMF (NHE).

	Eu^{III} **5**	$Eu^{III}-Cd^{II}$ **2**	$Eu^{III}-Ni^{II}$ **3**	$Eu^{III}-Zn^{II}$ **4**
$E_{1/2}^1$	−0.820	−0.995	−0.990	−1.165
$E_{1/2}^2$	-	−1.148	−1.520	−1.785
$E_{1/2}^3$	-	−1.340	−1.765	−1.959

reduction potentials of Eu^{III}/Eu^{II} are a function of the divalent ions in the second site and are negatively shifted relative to the mononuclear cryptate **5**, that is, Eu^{III} in mononuclear cryptate is reduced more easily than those in heteronuclear cryptates. The sequence of increasing difficulty of reduction in these cryptates has the order: mononuclear < Eu^{III}-Ni^{II} < Eu^{III}-Cd^{II} < Eu^{III}-Zn^{II}.

Crystal structure: A summary of the crystal data for complex **3** is given in Table 4. The structure of the complex cation $[EuNiL(dmf)]^{2+}$ of **3** is shown in Figure 3. The structural analysis of **3** confirms that the dinuclear $Eu^{III}-Ni^{II}$ entity exists in the cryptate. The Eu^{III} center is located at one end of the cavity and is eight-coordinate with bridgehead nitrogen atoms N(1), three imino-nitrogen atoms (N(2), N(3), N(4)), the oxygen atom O(4) of DMF, and three phenoxy-oxygen atoms (O(1), O(2), O(3)). The coordination configuration is best described as distorted dodecahedral. The average bond lengths for Eu^{III}–N(imino) (2.492 Å) and Eu^{III}–phenol (2.329 Å) in the heteronuclear cryptate **3** are shorter than those in mononuclear cryptate **5** (2.529 and 2.360 Å,[30] respectively), but the distance between the two bridgehead nitrogen atoms in **3** (9.112 Å) is longer than that in **5** (8.407 Å). These observations indicate that the Eu^{III} center needs to fine-tune its coordination environment to suit the coordination of Ni^{II}, with the result that the cryptand cycle is extended and a shortening of the coordination bonds of Eu^{III} takes place.

The other end of the cavity is occupied by Ni^{2+}. Three μ_2-phenolate-oxygen atoms and three imino-nitrogen atoms are coordinated to the Ni^{2+} center, forming a distorted octahedral configuration. The bond lengths of the three Ni–N(imino) and three Ni–O(phenol) bonds are in the ranges 2.055–2.104 Å and 2.091–2.218 Å, respectively, and the average angle of the three Eu^{III}-O(phenol)-Ni^{II} entities is 91.6°. The $Eu^{III}\cdots Ni^{II}$ distance (3.2204 Å) shows that a weak interaction exists between the Ni^{II} and Eu^{III} atoms. The Schiff-base cryptand H_3L is therefore a versatile ligand, capable of encapsulating monometal or heterodimetal ions.

Table 4. Crystallographic data for $[EuNiL(dmf)](ClO_4)_2\cdot MeCN$.

formula	$C_{41}H_{46}Cl_5N_{10}O_{12}EuNi$
M_r	1258.80
crystal system	monoclinic
space group	$P2(1)/c$
T [K]	293(2)
a [Å]	19.6676(5)
b [Å]	11.8492(3)
c [Å]	21.5154(6)
β	98.0300(10)
V	4964.9(2)
F_{000}	2536
Z	4
ρ_{calcd} [g cm^{-3}]	1.684
μ [mm^{-1}]	1.970
θ range for data collection [°]	$1.05 < \theta < 25.01$
$R_{(int)}$	0.0664
goodness of fit	1.196
number of data measured	20201
number of data with $I > 2\sigma(I)$	8659
R_1 ($I > 2\sigma(I)$)	0.0716
wR_2[a] ($I > 2\sigma(I)$)	0.1452

[a] $w = 1/[\sigma^2(F_o^2) + (0.03444P)^2 + 31.7350P]$, $P = [F_o^2 + 2F_c^2]/3$.

Luminescence properties: Excitation of mononuclear cryptate **5** and heteronuclear $EuI^{II}-M^{II}$ (M = Ca, Cd, Zn) cryptates in MeCN with light of wavelenght 400 nm gives rise to the characteristic emissions of the Eu^{3+} ion, and their emission spectra are essentially identical. By comparing the absorption and luminescence excitation spectra of the four cryptates at

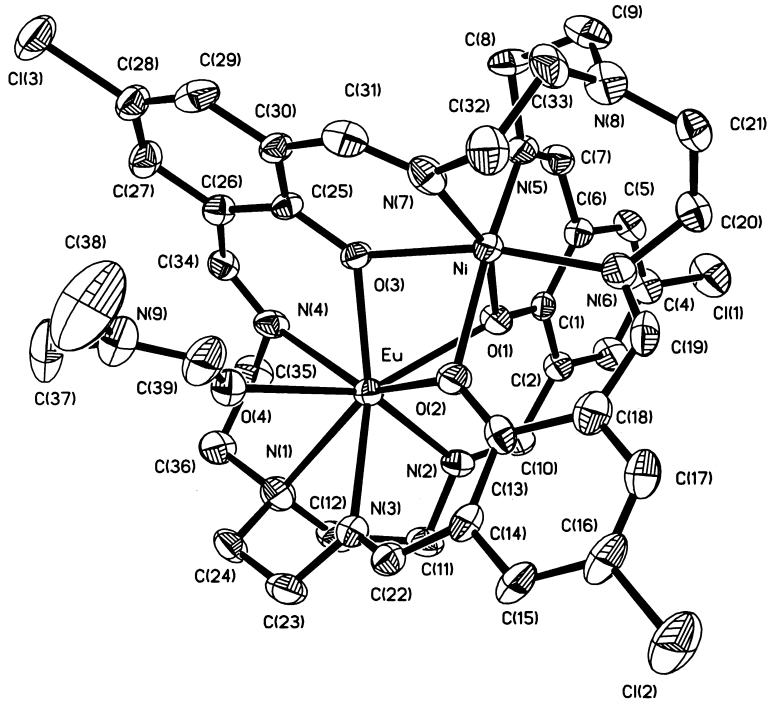

Figure 3. The crystal structure of the $[EuNiL(dmf)]^{2+}$ ion in **3**. Selected bond lengths [Å] angles [°]: Eu–O(1) 2.340(6), Eu–O(2) 2.335(6), Eu–O(3) 2.313(5), Eu–O(4) 2.403(7), Eu–N(1) 2.653(8), Eu–N(2) 2.499(8), Eu–N(3) 2.500(8), Eu–N(4) 2.477(8), Ni–O(1) 2.140(6), Ni–O(2) 2.218(6), Ni–O(3) 2.091(5), Ni–N(5) 2.104(8), Ni–N(6) 2.055(8), Ni–N(7) 2.093(9); Ni-O(1)-Eu 91.8(2), Ni-O(2)-Eu 90.0(2), Ni-O(3)-Eu 93.9(2).

about 400 nm, one evident similarity between them is that they show energy transfer from an excited state to the Eu^{III} vibration level. All emissions arise from the $^5D_0$ level corresponding to the $^5D_0 \rightarrow {}^7F_J$ ($\Delta J = 0, 1-4$) transition. The positions of the bands do not change significantly on addition of the second metal ion to the mononuclear cryptate, implying that there is no change in the coordination environment of the Eu^{III} ion. The emission spectra of cryptates **1**, **4**, and **5** are shown in Figure 4.

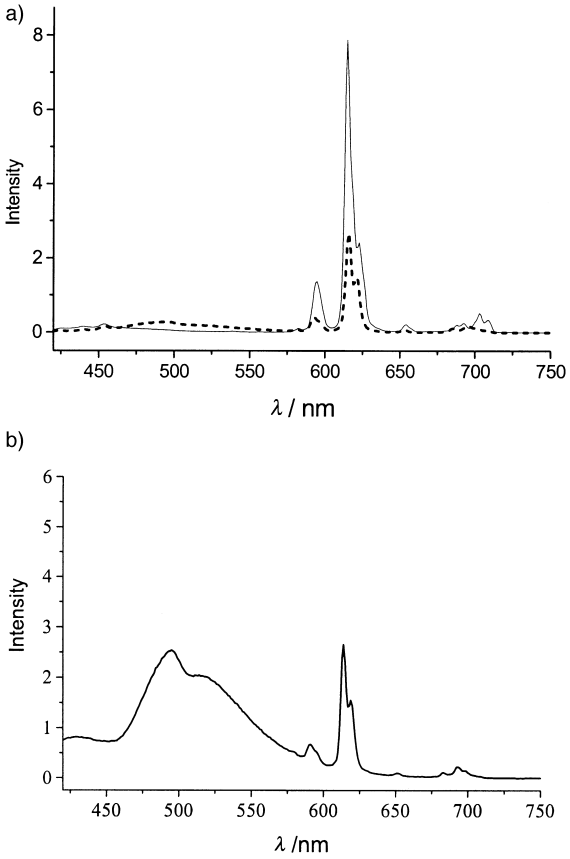

Figure 4. The emission spectra of a) mononuclear **5** (dash line) and **4** (full line), b) **1**; concentration: 4.0×10^{-6} mol L^{-1} in MeCN. The response of the detector was corrected.

The weak bands at 580 nm ($^5D_0 \rightarrow {}^7F_1$) and the intense bands around 613 nm ($^5D_0 \rightarrow {}^7F_2$) are magnetic dipole-allowed and electric dipole-allowed transitions, respectively. The emission intensities of the latter are sensitive to the coordination environment of the Eu^{III} ion. The intensities for the $^5D_0 \rightarrow {}^7F_2$ transition are much higher than those for $^5D_0 \rightarrow {}^7F_1$, showing that these cryptates have no inversion center. The bands around 655 and 700 nm were produced from the transitions $^5D_0 \rightarrow {}^7F_3$ and $^5D_0 \rightarrow {}^7F_4$, respectively.

On comparing the fluorescence spectra of the mononuclear cryptate **5** with those of the heteronuclear cryptates, it is found that the emission intensity of **5** is weaker than those of **2** and **4**, and close to that of **1**. The intensity ratio of **2** or **4** to **5** is about 3:1. The order of increasing of emission intensities is in agreement with that of quantum yields. The sequence is: mononuclear < Eu^{III} – Ca^{II} < Eu^{III} – Cd^{II} < Eu^{III} – Zn^{II}.

A broad band around 450–575 nm corresponding to a ligand-centered band is observed for each cryptate. The ligand-centered band of cryptate **1** displays two maxima at 496 and 521 nm, which result from partial dissociation of calcium ions in the solution, as proven by ES-MS. It is remarkable that both the emission intensity and quantum yield of the ligand of cryptate **1** are the highest among the heterodinuclear complexes, but those of Eu^{III} in **1** are lower than those of **2** and **4**. The quantum yield of the Eu^{III} ion in cryptate **1** was close to that of the mononuclear Eu^{III} cryptate **5**, implying that the Ca^{2+} ion made little contribution to the luminescence of Eu^{III} in **1**, but made a contribution to that of the ligand. The light absorbed by the ligand of **1** is therefore not converted efficiently into light emitted by Eu^{III}.

The quantum yields and lifetimes of cryptates at 613 nm are listed in Table 5. Cryptate **4** has the highest quantum yield for Eu^{III} emission of the compounds studied. The ratio of **4** or **2** to that of **5** is 1.90:1 or 1.73:1, indicating that the synergism of

Table 5. Luminescence quantum yields and lifetimes of some Eu^{III} cryptates in MeCN at 293 K.[a]

Cryptate	$\Phi_{Eu^{III} \times 10^2}$	$\Phi_L \times 10^2$	τ [ms][b]
1	1.50	3.74	0.45
2	2.46	0.43	0.46
4	2.76	0.32	0.29
5	1.42	0.91	0.29

[a] Experimental errors of Φ and τ are 10% and 0.01 ms, respectively. The data are averages of at least three independent determinations. [b] The lifetimes were measured at 613 nm.

Zn^{II} or Cd^{II} ions with Eu^{III} increased the efficiency of energy transfer between the triplet level of the ligand and the $^5D_0$ excited state of the Eu^{III} ion. The enhancement of emission of the Eu excited state resulting from the binding of Zn^{II} or Cd^{II} ions is likely to be related to suppression of photo-induced electron transfer from the ligand to the Eu center. Such an effect has been used to "sense" zinc.[37] In addition, the Eu^{III} ion in cryptate **4** has the most negative potential obtained from cyclic voltammetry. It is so difficult to reduce Eu^{III} after introduction of Zn^{II} that deactivation is greatly decreased for the $^5D_0$ emitting level of Eu^{III}.[17, 22] Moreover in [Eu(H_3L)(NO_3)(H_2O)](ClO_4)$_2$ (**5**), the labile coordinated nitrate ion and encapsulated water molecule in the macrocylcic cavity were replaced in each case by a second metal ion which prevented interaction of the Eu^{III} ion with solvent molecules.

For cryptate **3**, no emission bands of Eu^{III} are observed. The fluorescenece of **3** is quenched by energy transfer from the excited Eu^{III} to Ni^{II} through the bridging oxygen atoms followed by a radiationless energy loss, as reported by others.[38]

Recently, many investigations have been done on cryptation-enhanced fluorescence to make chemosensors.[17, 31] We use mononuclear Eu^{III} cryptate as a receptor (host molecule) and input a second metal ion as guest species into the host molecule, resulting in a change in the fluorescence intensity of Eu^{III}. The intensities of Eu^{III} can be tuned by the selective introduction of metal ions into the receptor. Herein, long wavelength excitation was used, one of the longest used to

0947-6539/02/0817-3988 $ 20.00+.50/0 *Chem. Eur. J.* **2002**, *8*, No. 17

date. Because the excitation wavelength used is below 320 nm, direct application of such systems is clearly precluded.[39] Such a cryptand-based fluorescence system might be useful for the development of photonic devices and metal ion sensors in the future.

Conclusion

Four new heterodinuclear cryptates $[EuML(dmf)](ClO_4)_2$ (M = Ca, Cd, Ni, Zn) were synthesized by a two-step method. $[Eu(H_3L)(NO_3)(H_2O)](ClO_4)_2$ is used as the precursor. The $[EuCaL]^{2+}$ ion acted as an intermediate in the reaction process, being formed by the addition of CaH_2 to the reaction solution to adjust the pH value. ES-MS shows that the $[EuCaL]^{2+}$ ion is unstable and labile toward dissociation and replacement of the Ca^{2+} ion. X-ray analysis indicates that a strict dinuclear $Eu^{III}-Ni^{II}$ entity exists in the cryptates. After the formation of $Eu^{III}-Ni^{II}$ cryptate, the Eu–N(imino) and Eu–O(phenol) bond lengths are shortened because the environment surrounding the Eu^{III} ion was slightly modified to suit the coordination of the Ni^{2+} ion.

The introduction of a second metal ion into the mononuclear Eu^{III} cryptate resulted in a blue shift of the three ligand-centered bands and a small increase in the molar absorption coefficients. In addition, a negative shift of the redox potential of Eu^{III}, and a change in luminescence intensity of Eu^{III} took place. It is remarkable that the introduction of the Ni^{2+} ion led to quenching of the Eu^{III} emission by energy transfer from the excited Eu^{III} to Ni^{II}. Conversely, introduction of Zn^{2+} or Cd^{2+} into mononuclear Eu^{III} cryptate led to a threefold increase of the luminescence intensity of Eu^{III}. However, the introduction of Ca^{2+} led to a clear increase of the emission of ligand-centered bands, but the emission of Eu^{III} hardly changed because the light absorbed by the ligand was not converted efficiently into light emitted by Eu^{III} in presence of Ca^{2+}. The order of increase in quantum yield of Eu^{III} is: mononuclear < Eu–Ca < Eu–Cd < Eu–Zn.

Experimental Section

Materials: $Eu(NO_3)_3 \cdot 6H_2O$ was prepared by dissolving Eu_2O_3 (99.99%) in an excess of nitric acid; tris(2-aminoethyl)amine and 2,6-diformyl-4-chlorophenol were prepared by literature methods.[40] Acetonitrile for the fluorescence study was dried by treatment with CaH_2 and distilled over P_2O_5. The $[Ru(bipy)_3]Cl_2$ used as a standard material in the quantum yield measurement was synthesized according to a literature procedure[41] and recrystallized twice from doubly distilled water. The quantum yield was checked against rhodamine B[42] and found to be in accord with the literature value.

Physical measurements: C, H, and N elemental analyses were performed on a Perkin-Elmer 240c analytical instrument. The metal–element analysis was performed on a POEMS (II) (ICP-MS) instrument. The molar electrical conductivities of the complexes (10^{-4} mol L^{-1}) in DMF were measured at 25 °C ± 0.1 °C using a BSD-A conductmeter. The IR spectra were recorded as KBr discs using a Nicolet 5 DX FTIR spectrophotometer. Electronic spectra were recorded on a UV-3100 spectrophotometer. The electrospray mass spectra were determined on a Finnigan LCQ mass spectrometer, the concentration of the samples being about 1.0 μmol L^{-1}. The diluted solutions were electrosprayed at a flow rate of 5×10^{-6} L^{-1} min^{-1} with a needle voltage of +4.5 KV. The mobile phase was methanol.

Cyclic votammetry experiments were performed on a PAR Model 273 potentiostat coupled to a PAR Model 175 universal programmer. A three-electrode system was used in all experiments. A glassy carbon electrode was employed as the working electrode, Ag–AgCl as reference electrode and a platinum coil wire as auxiliary electrode. Ferrocene was used as the internal standard. It has been proposed that the oxidation of ferrocene to the ferrocenium ion occurs at the same potential in some solvents. In water the process occurs at +0.400 V versus NHE or at 0.160 V versus SCE.[43] Experiments were performed under a purified nitrogen atmosphere at 25 ± 0.1 °C. The complex concentrations were 1.5×10^{-3} mol L^{-1} in 0.1 mol L^{-1} TBAP (tetrabutylammonium perchlorate) DMF solutions. The solutions were deaerated for about 15 min before applying the voltage. The half wave potentials $E_{1/2}$ were calculated approximately from $(E_{pa} + E_{pc})/2$ and the error in the measured potential was ±2 mV. Unless otherwise stated, all potentials reported are referenced to NHE.

Luminescence measurements: Luminescence spectra were measured with an AB2 spectrafluorometer. In measurements of emission and excitation spectra the band pass was 5.0 nm. The quantum yield of Eu^{III} complexes was measured by using a relative method with $[Ru(bipy)]Cl_2$ as the standard. Its quantum yield is 0.042 in aqueous solution at 20 °C.[44] The quantum yields of the Eu^{III} complexes were calculated from Equation (1), where Φ is the quantum yield, subscript s stands for the reference and x for sample, A is the absorbance at the excitation wavelength (400 nm), n is the reference index (1.343 for MeCN solution and 1.344 for aqueous solution) and D is the emission integrated area in the emission range of 575–725 nm.

$$\Phi_x/\Phi_s = [A_S/A_x][n_x^2/n_s^2][D_x/D_s] \quad (1)$$

The sample absorbances (A_{ex}) at the excitation wavelength were kept as low as possible to avoid fluorescence errors ($A_{exc} = 0.09-0.11$). The solutions, containing complexes at concentrations of about 2.0×10^{-6} mol L^{-1}, were deoxygenated with a stream of super-pure nitrogen for 15 min.

The fluorescence lifetimes of the complexes at 613 nm were measured by using a laser-induced fluorescence method. The excitation source is a Q-switched Nd:YAG laser with a pulse-width of 10 ns and a repetition rate of 10 Hz. The samples were excited at a wavelength of 355 nm and fluorescence signals were aggregated into a 0.6 m monochromator using a lens. Detected data were averaged on a 500 MHz digital real-time oscilloscope (Tektronix, TDS 620B).

Crystal structure determination: Single crystals of $[EuNiL(dmf)](ClO_4)_2 \cdot$ MeCN (**3**) were obtained by a slow diffusion of diethyl ether vapor into a solution of the cryptate in acetonitrile for one week. Diffraction data were collected on a Siemens Smart/CCDC area-detector[45] with monochromated $Mo_{K\alpha}$ ($\lambda = 0.71073$ Å) radiation using Φ and ω scans. The collected data were reduced by using the program SAINT and empirical absorption correction was done using the SADABS[46] program. The structure was solved by direct methods. All non-hydrogen atoms were refined anisotropically by full-matrix least-squares methods. Hydrogen atoms of the ligands were placed in their calculated positions with C–H = 0.93 Å. All hydrogen atoms were assigned fixed isotropic thermal parameters (1.2 times the atoms to which they were attached) and were allowed to ride on their respective parent atoms. The contribution from these hydrogen atoms was included in structure-factor calculations. All computations were carried out using the SHELXTL-PC program package.[47]

CCDC-189333 contains the supplementary crystallographic data for this paper. These data can be obtained free of charge via www.ccdc.can.ac.uk/conts/retrieving.html (or from the Cambridge Crystallographic Centre, 12 Union Road, Cambridge CB2 1EZ, UK; Fax: (+44) 1223-336033; or deposit@ccdc.cam.ac.uk).

Syntheses of the cryptates

$[EuCaL(dmf)](ClO_4)_2$ (1): $[Eu(H_3L)(NO_3)(H_2O)](ClO_4)_2$ (**5**; see below) (0.120 g, 0.1 mmol) was dissolved in methanol (15 mL) with a small amount of DMF (1.0 mL). Solid CaH_2 (0.012 g, 0.3 mmol) was added to the solution, and the resultant solution was stirred for 30 min, and then filtered. The light yellow microcrystals of **1** were obtained by evaporating the filtrate at room temperature. Yield: 0.079 g, 65%; IR (KBr): $\tilde{\nu} = 1648$ (s, C=N), 1542 (s, C–O), 1090 (s, ClO_4^-), 625 cm^{-1} (m, ClO_4^-); Λ_m (DMF,

298 K): 140 $S cm^2 mol^{-1}$; elemental analysis calcd (%) for $C_{39}H_{43}Cl_5N_9O_{12}$CaEu: C 39.06, H 3.62, N 10.51, Eu 12.67, Ca 3.34; found: C 39.38, H 3.79, N 10.62, Eu 12.89, Ca 3.49.

[EuCdL(dmf)](ClO$_4$)$_2$ (2): The mononuclear europium(III) cryptate **5** (0.120 g, 0.1 mmol) was dissolved in methanol (15 mL) with a small amount of DMF (1.0 mL). After the addition of an excess of solid CaH_2 and stirring for 2 h, the pH of the solution changed to 7–8. Calcium(II) perchlorate (0.031 g, 0.1 mmol) was added to the solution and the mixture was refluxed for about 4 h. The solution was concentrated until the red product formed. Yield: 0.077 g, 60%; IR (KBr): $\tilde{\nu} = 1643$ (s, C=N), 1541 (s, C–O), 1089 (s, ClO_4^-), 625 cm^{-1} (m, ClO_4^-); Λ_m (DMF, 298 K): 142 $S cm^2 mol^{-1}$; elemental analysis calcd (%) for $C_{39}H_{43}Cl_5N_9O_{12}$CdEu: C 36.82, H 3.41, N 9.91, Cd 8.84, Eu 11.95; found: C 36.72, H 3.54, N 9.80, Cd 8.76, Eu 11.98.

[EuNiL(dmf)](ClO$_4$)$_2$·MeCN (3): This compound was synthesized by methods similar to those used in the synthesis of **2**. Yield: 0.057 g, 45%; IR (KBr): $\tilde{} = 1645$ (s, C=N), 1541 (s, C–O), 1089 (s, ClO_4^-), 625 cm^{-1} (m, ClO_4^-); Λ_m (DMF, 298 K): 145 $S cm^2 mol^{-1}$; elemental analysis calcd (%) for $C_{41}H_{46}Cl_5N_{10}O_{12}$EuNi: C 39.12, H 3.69, N 11.13, Eu 12.07, Ni 4.66; found: C 39.25, H 3.76, N 10.89, Eu 11.89, Ni 4.78.

[EuZnL(dmf)](ClO$_4$)$_2$·MeCN (4): This compound was synthesized by methods similar to those used in the synthesis of **2**. Yield: 0.073 g; 58%; IR (KBr): $\tilde{\nu} = 1645$ (s, C=N) 1541 (s, C–O), 1089 (s, ClO_4^-), 625 cm^{-1} (m, ClO_4^-); Λ_m (DMF, 298 K): 145 $S cm^2 mol^{-1}$; elemental analysis calcd (%) for $C_{41}H_{46}Cl_5N_{10}O_{12}$EuZn: C 38.79, H 3.66, N 11.03, Eu 11.97, Zn 5.46; found: C 39.25, H 3.76, N 10.89, Eu 11.89, Zn 5.34.

[Eu(H$_3$L)(NO$_3$)(H$_2$O)](ClO$_4$)$_2$ (5): This compound was synthesized as described in reference [30].

Acknowledgements

This project was supported by the National Natural Science Foundation of China, Foundation of FuZhou State Key Laboratory of Structure Chemistry, and Foundation of State Key Laboratory of Lanthanide Chemistry, Beijing University.

[1] a) V. Alexander, *Chem. Rev.* **1995**, *95*, 237–342; b) L. di Bari, G. Pintacuda, P. Salvadori, R. S. Dickins, D. Parker, *J. Am. Chem. Soc.* **2000**, *122*, 9257–9264.
[2] C. Piguet, J.-C. G. Bunzli, *Chem. Soc. Rev.* **1999**, *28*, 347–358.
[3] a) J.-M. Lehn, *Angew. Chem.* **1990**, *102*, 1347—1362; *Angew. Chem. Int. Ed. Engl.* **1990**, *29*, 1304–1319; b) Y. Bretonniere, M. Mazzanti, J. Pecaut, F. A. Dunand, A. E. Merbach, *Chem. Commun.* **2001**, 621–622.
[4] C.-J. Feng, Q.-H. Luo, C.-Y. Duan, M.-C. Shen, Y.-J. Liu, *J. Chem. Soc. Dalton Trans* **1998**, 1377–1380.
[5] M. G. B. Drew, O. W. Howarth, C. J. Harding, N. Martin, J. Nelson, *J. Chem. Soc. Chem. Commun.* **1995**, 903–905.
[6] J.-J. Zhang, W. Zhang, Q.-H. Luo, Y.-H. Mei, *Polyhedron* **1999**, *18*, 3637–3642.
[7] G. R. Choppin, D. R. Peterman, *Coord. Chem. Rev.* **1998**, *174*, 283–299.
[8] S. Aime, M. Botta, M. Fasano, E. Terreno, *Chem. Soc. Rev.* **1998**, *27*, 19–30.
[9] A. Rizzi, R. Baggio, R. Calvo, M. T. Garland, O. Pena, M. Perec, *Inorg. Chem.* **2001**, *40*, 3623–3625.
[10] a) B. Hofmann, A. Bogdanov, E. Marecos, W. Semmlerand, R. Weissleder, *J. Magn. Reson. Imaging* **1999**, 9, 336; b) A. Beeby, I. Clarkson, S. Faulkner, S. Botchway, D. Parker A. W. Parker, *J. Photochem. Photobiol. B* **2000**, *57*, 83.
[11] a) P. Ghosh, P. K. Bharadwaj, J. Roy, S. Ghosh, *J. Am. Chem. Soc.* **1997**, *118*, 11903–11909; b) T. Gunnlaugsson, D. A. McDonnailland, D. Parker, *Chem. Commun.* **2000**, 93–94.
[12] W. T. Carnall, in *Handbook on the Physical and Chemistry of Rare Earths, Vol. 3* (Ed. K. A. Gschneidner.Jr., L. Eying), Elsevier, Amsterdam, **1987**, p. 171.
[13] D. Parker, J. A. G. Williams, *J. Chem. Soc. Dalton Trans.* **1996**, 3613–3628.
[14] C. Piguet, C. Edder, S. Rigault, G. Bernardinelli, J.-C. G. Bunzli, G. Hopfgartner, *J. Chem. Soc. Dalton Trans.* **2000**, 3999–4006.
[15] C. Edder, C. Piguet, J.-C. G. Bunzli, G. Hopfgartner, *Chem. Eur. J.* **2001**, *7*, 3014–3020.
[16] R. D. Archer, H. Chen, *Inorg. Chem.* **1998**, *37*, 2089–2095.
[17] N. Sabbatini, M. Guardigi, *Coord. Chem. Rev.* **1993**, *123*, 201–228.
[18] S. Petoud, J.-C. G. Bunzli, T. Ganzman, C. Piguet, Q. Xiang, P. R. Thummel, *J. Luminescence* **1999**, *82*, 69–79.
[19] S.-X. Wang, Y. Zhu, Y.-X. Cui, L.-F. Wang, Q.-H. Luo, *J. Chem. Soc. Dalton Trans.* **1994**, 2523–2530.
[20] S.-X. Wang, Q.-H. Luo, X.-X. Zhou, Z.-Z. Zeng, *Polyhedron* **1993**, 1939–1945.
[21] C. Bazzicalupi, A. Bencini, A. Bianchi, C. Giorgi, V. Fusi, A. Masotti, B. Valtancoli, A. Roque, F. Pina, *Chem. Commun.* **2000**, 561–562.
[22] B. Alpha, E. Anklam, R. Deschenaux, J.-M. Lehn, M. Pietraszkiewicz, *Helv. Chem. Acta* **1998**, *77*, 1042–1052.
[23] J.-M. Lehn, M. Pietraszkiewicz, J. Karpiuk, *Helv. Chim. Acta* **1990**, *73*, 106–111.
[24] L. Prodi, M. Maestri, R. Ziessi, V. Balzani, *Inorg. Chem.* **1991**, *30*, 3798–3802.
[25] N. Sabbatini, M. Guardigilli, I. Manet, F. Bolletta, *Inorg. Chem.* **1994**, *33*, 955–959.
[26] A. Dossing, H. Toftlund, A. Hazell, J. Bourassa, P. C. Ford, *J. Chem. Soc. Dalton Trans* **1997**, 335–339.
[27] P. Gawryszewska, L. Jerzykiewicz, M. Pietraszkiewicz, J. Legendziewicz, J. P. Riehl, *Inorg. Chem.* **2000**, *39*, 5365–5372.
[28] F. J. Steemer, W. Verboom, D. N. Reinhoudt, E. B. Van Der Tol, J. W. Verhoeven, *J. Am. Chem. Soc.* **1995**, *117*, 9408–9114.
[29] C. Platas, F. Avecilla, A. de Blas, T. Rodriguez-Blas, C. F. G. C. Geraldes, E. Toth, A. E. Merbach, J.-C. G. Bunzli, *J. Chem. Soc. Dalton Trans* **2000**, 611–618.
[30] Q.-Y. Chen, C.-J. Feng, Q.-H. Luo, C.-Y. Duan, X.-S. Yu, D.-J. Liu, *Eur. J. Inorg. Chem.* **2001**, 1063–1069.
[31] C. Galaup, C. Picard, B. Cathala, L. Cazaux, P. Tisnes, H. Autiero, D. Aspe, *Helv. Chim. Acta* **1999**, *82*, 543–560.
[32] R. E. P. Winpenny, *Chem. Soc. Rev.* **1998**, *27*, 447–452.
[33] Q.-Y. Chen, Q.-H. Luo, Z.-L. Wang, J.-T. Chen, *Chem. Commun.* **2000**, 1033–1034.
[34] Q.-Y. Chen, Q.-H. Luo, L.-M. Zheng, Z.-L. Wang, J.-T. Chen, *Inorg. Chem.* **2002**, 41, 603–605.
[35] B. Bosnich, *Inorg. Chem* **1999**, *38*, 2554–2562.
[36] J. D. Tee, *Talanta* **1973**, *20*, 1029–1038.
[37] O. Reany, T. Gunnlaugsson, D. Parker, *J. Chem. Soc. Perkin Trans.* **2000**, 1819–1831.
[38] M. Sakamoto, K. Yamamoto, K. Matsumoto, Y. Nishida, H. Okawa, *Bull. Chem. Soc. Jpn.* **1994**, *67*, 2707–2711.
[39] A. Beeby, S. Faulkner, D. Parker, J. A. G. Williams, *J. Chem. Soc. Perkin Trans.* **2001**, 1268–1273.
[40] a) S. Taniguchi, *Bull. Chem. Soc. Jpn.* **1984**, *57*, 2683–2684; b) E. Kimura, S. Young, J. P. Collman, *Inorg. Chem.* **1970**, *9*, 118–124.
[41] F. H. Burstall, *J. Chem. Soc.* **1936**, *1*, 173–175.
[42] K. Nakamaru, *Bull. Chem. Soc. Jpn.* **1982**, *55*, 2697–2705.
[43] R. R. Gagne, C. A. Koval, G. C. Lisensky, *Inorg. Chem.* **1984**, *19*, 2855–2857.
[44] J. V. Houten, R. J. Watts, *J. Am. Chem. Soc.* **1976**, *98*, 4853–4858.
[45] G. M. Sheldrick, SAINT (version 4), Siemens Analytical X-ray Systems, Inc., Madison, Wisconsin, USA, **1994**.
[46] G. M. Sheldrick, SADABS, Absorption Correction Progam, University of Göttingen, Germany, **1996**.
[47] G. M. Sheldrick, SHELXTL (version 5.0), Siemens Analytical X-ray systems, Inc., Madison, Wisconsin, USA, **1997**.

Received: January 22, 2002
Revised: May 7, 2002 [F3815]

  0947-6539/02/0817-3990 $ 20.00+.50/0